◆ Human Brain Mapping 37:2755–2766 (2016) ◆

Correlated Inter-Regional Variations in Low Frequency Local Field Potentials and Resting State BOLD Signals Within S1 Cortex of Monkeys

George H. Wilson III,[1,2] Pai-Feng Yang,[1,2] John C. Gore,[1,2] and Li Min Chen[1,2]*

[1]*Vanderbilt University Institute of Imaging Science, Nashville, Tennessee*
[2]*Department of Radiology and Radiological Sciences, Vanderbilt University Medical Center, Nashville, Tennessee*

Abstract: The hypothesis that specific frequency components of the spontaneous local field potentials (LFPs) underlie low frequency fluctuations of resting state fMRI (rsfMRI) signals was tested. The previous analyses of rsfMRI signals revealed differential inter-regional correlations among areas 3a, 3b, and 1 of primary somatosensory cortex (S1) in anesthetized monkeys (Wang et al. [2013]: Neuron 78:1116–1126). Here LFP band(s) which correlated between S1 regions, and how these inter-regional correlation differences covaried with rsfMRI signals were examined. LFP signals were filtered into seven bands (delta, theta, alpha, beta, gamma low, gamma high, and gamma very high), and then a Hilbert transformation was applied to obtain measures of instantaneous amplitudes and temporal lags between regions of interest (ROI) digit–digit pairs (areas 3b–area 1, area 3a–area 1, area 3a–area 3b) and digit–face pairs (area 3b–face, area 1–face, and area 3a–face). It was found that variations in the inter-regional correlation strengths between digit–digit and digit–face pairs in the delta (1–4 Hz), alpha (9–14 Hz), beta (15–30 Hz), and gamma (31–50 Hz) bands parallel those of rsfMRI signals to varying degrees. Temporal lags between digit–digit area pairs varied across LFP bands, with area 3a mostly leading areas 1/2 and 3b. In summary, the data demonstrates that the low and middle frequency range (1–50 Hz) of spontaneous LFP signals similarly covary with the low frequency fluctuations of rsfMRI signals within local circuits of S1, supporting a neuronal electrophysiological basis of rsfMRI signals. Inter-areal LFP temporal lag differences provided novel insights into the directionality of information flow among S1 areas at rest. *Hum Brain Mapp 37:2755–2766, 2016.*

Key words: resting state functional connectivity; LFP; fMRI; somatosensory cortex; non-human primate

INTRODUCTION

The identification of patterns of highly correlated low frequency MRI signals in the resting state (termed resting state functional connectivity) has influenced greatly our view of the functional organization of the brain at rest, and provides a powerful approach to delineate and describe functional neural circuits [Bisal et al., 1995; Deco et al., 2011; Deco and Corbetta, 2011; Fingelkurts and Kahkonen, 2005; Fox and Raichle, 2007; Greicius et al., 2002; Guye et al., 2008; Gusnard & Raichle 2001]. Resting state fMRI data are relatively easy to collect and have

Contract grant sponsor: NIH grants; Contract grant numbers: NS078680 (JCG) and NS069909 (LMC)

*Correspondence to: Li Min Chen, MD, PhD, Associate Professor, Department of Radiology and Radiological Sciences, Institute of Imaging Science, Vanderbilt University Medical Center, 1161 21st Ave. S., AA 1105 MCN, Nashville, TN. E-mail: limin.chen@vanderbilt.edu

Received for publication 14 December 2015; Revised 14 March 2016; Accepted 23 March 2016.

DOI: 10.1002/hbm.23207

Published online 19 April 2016 in Wiley Online Library (wileyonlinelibrary.com).

become popular particularly for studies on patient populations. Observations of altered resting state connectivity in several disorders suggest these correlations represent an important level of neural organization and may play a fundamental role in the execution and maintenance of various brain functions [Damoiseaux, 2012; Fox and Greicius, 2010].

The interpretation of event related and resting state fMRI findings relies on our understanding of the relationships between fMRI signals and the underlying neurophysiology. Thus far, such information is quite limited, and there have been few studies that attempt to validate our interpretation of resting state correlations as indicating anatomical connectivity or as being directly related to synchronous electrical activity. To date, reports about the precise relationships between BOLD signals and electrophysiological activity with stimulation or at rest have been inconsistent. In stimulation or task conditions, some studies have found strong correlation between BOLD responses and power in the gamma band (30–150 Hz) of LFP signals [Logothetis et al., 2001; Mukamel et al., 2005; Shmuel et al., 2006]. In a resting state, while some evidence suggests that slow changes in the gamma band of LFP signals contribute to the spontaneous fluctuations in BOLD signal [He et al., 2008; Niessing et al., 2005; Nir et al., 2007, 2008], others suggest that lower power bands (<20 Hz) predominantly contribute to changes in BOLD signal [Lu et al., 2007; Wang et al., 2012]. To date, no studies have examined the relationships between BOLD and electrophysiological signals within a meso-scale local functional network, such as the digit–face representation regions within sub-regions of the primary somatosensory (S1) cortex (area 3a, area 3b, area 1) of non-human primates.

This study aims to address this issue using the well-characterized digit–face functional connectivity model in new world monkeys. Our previous observations showing that distinct intrinsic functional connections exist among different sub-regions of the primary somatosensory cortex (S1) of squirrel monkeys [Wang et al., 2013] lead us to believe that inter-areal correlation differences between different region of interest (ROI) pairs may be a sensitive measure for examining the underlying neuronal activity of resting state fMRI signals. Using the same experimental model, we test our hypothesis that specific components (frequency bands) of the local field potential (LFP) underlie the fluctuations of low frequency rsfMRI signals. In this study we quantified the inter-regional correlation differences in simultaneously recorded LFP signals from digit representations in S1 sub-region areas 3a, 3b, and 1/2, as well as a control face region in area 3b, to compare their inter-areal correlation strengths with those of rsfMRI signals directly in individual monkeys. We found that inter-regional correlation differences in delta, alpha, beta, and low gamma bands (1–50 Hz) of local field potentials agree well with the inter-regional correlation of resting state fMRI signals. Additionally, temporal lags between LFP signals of different ROI pairs varied, suggesting the information flow between S1 sub-regions differ across bands of local field potentials at rest.

EXPERIMENTAL PROCEDURE

Animal Preparation

Two squirrel monkeys (*Saimiri sciureus*) were included in this study and went through functional imaging and microelectrode electrophysiological mapping and recording sessions. Animals were initially sedated with ketamine hydrochloride (10 mg/kg)/atropine (0.05 mg/kg) and then maintained with isoflurane anesthesia (0.6%–1.1%) delivered in a 70:30 O_2/N_2O mixture. Animals were artificially ventilated to maintain an end-tidal CO_2 of 4%. Rectal temperature was maintained at 37.5°C–38.5°C. Heart rate and respiration pattern were continuously monitored and recorded. All procedures were in compliance with and approved by the Institutional Animal Care and Use Committee of Vanderbilt University.

MRI Methods and Analysis

All MRI scans were performed on a 9.4-T Varian Inova spectrometer (Varian Medical Systems) using a 3-cm surface coil. T2-weighted oblique structural images (echo time [TE], 16 ms; repetition time [TR], 200 ms) at $0.078 \times 0.078 \times 2$ mm^3 resolution were acquired and later used as the reference for coregistration with fMRI maps and with blood-vessel maps in which microelectrode penetration sites were marked. Functional MR images were acquired with the same image slice prescription using a gradient echo (GE) planar sequence (TE, 19 ms; TR, 1.5 s) at voxel sizes of $0.55 \times 0.55 \times 2$ mm^3. Within each imaging session (day), resting-state BOLD fMRI data acquisition consisted of several 7.5 min long runs. Each run contained 300 imaging volumes. A total of eight resting-state fMRI runs were acquired from two monkeys and included in the analysis. Resting state functional echo planar imaging (EPI) data underwent standard pre-processing steps and were then analyzed using the AFNI software package. The RETROICOR method [Glover et al., 2000] was used to correct for physiological noise using the respiration pattern recorded during the scans. Slice timing correction was performed following the slice-by-slice motion correction. Six translation and rotation parameters along with the global signal were used to regress out temporal variations caused by motion and hardware related signal baseline drift. Spatial smoothing of the data was then performed using a Gaussian kernel with full width at half max (FWHM) = 0.8 mm followed by temporal smoothing with a band-pass filter with cutoff frequencies at 0.01 and 0.1Hz (fslmaths, FSL).

A single voxel seed ROI was selected in each of areas 3a, 3b, and 1 within a single digit region (e.g., digit 2 in area 3b and area 1) and one control ROI seed was chosen in the face region of area 3b based on an electrophysiologically

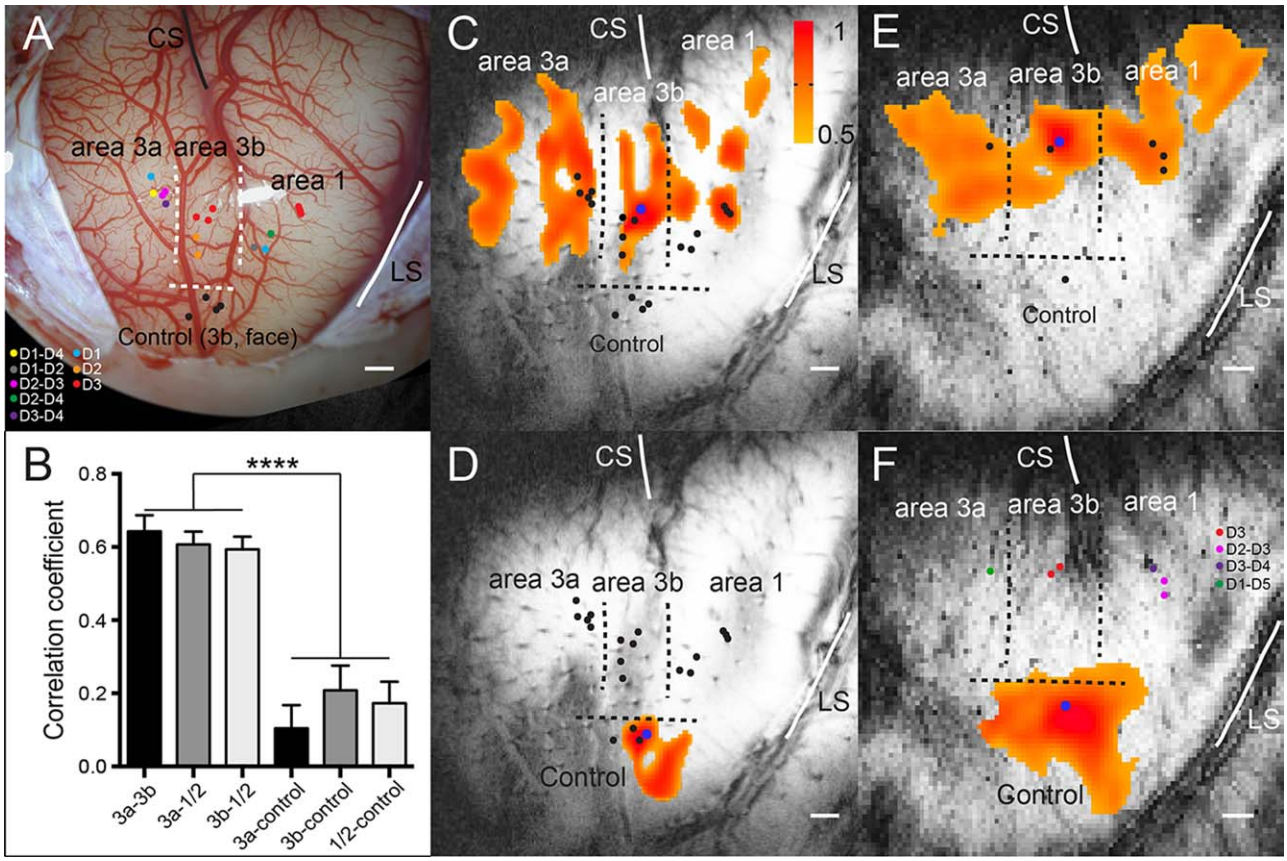

Figure 1.

Functional connectivity revealed by resting state fMRI signals within S1 subregions (areas 3a, 3b, 1/2) of squirrel monkeys. (**A**) Electrophysiological map (blood vessel map) of S1 cortex (areas 3a, 3b, 1/2) of subject SM-H with dots indicating electrode penetration sites, where neurons with receptive fields on palm, digits, and face were isolated in subject SM-H. CS: central sulcus. LS: lateral sulcus. *Dotted lines* represent estimated inter-areal borders between areas 3a, 3b, and 1/2, and between digit and face. *Color dots* indicate the microelectrode penetration sites and the receptive fields of the neurons isolated at each site. (**B**) Bar plots show correlation coefficient values between three S1 digit ROI pairs: area 3a and area 3b (3a–3b), area 3a and area 1/2 (3a–A1), and area 3b and area 1/2 (3b–A1); and between S1 digit sub-regions and control area 3b face region: area 3a and control (3a–control), area 3b and control (3b–control) and area 1/2 and control (A1–control). ****$p < 0.0001$. (**C and D, E and F**) The connectivity maps of seeds (*blue dots*) in area 3b digit 3 (D3) and control face locations in subjects SM-H and SM-R, respectively. The connectivity maps were presented with threshold of $r > 0.5$. Scale bar represents 1 mm.

defined digit representation map of each animal. Pair-wise inter-regional (ROI) correlation analyses were conducted to evaluate the strengths of functional connectivity between different ROI pairs (Fig. 1B). Correlation coefficients (r values) between ROI pairs were calculated, and then averaged across runs ($n = 8$, from 3 sessions in 2 animals) for comparisons (Fig. 1B). Voxel wise correlation maps were thresholded at $r \geq 0.5$, and then spatially interpolated onto high-resolution structural images for display (Fig. 1C–F).

Electrophysiological Recording and Analysis

Multi-site simultaneous microelectrode recordings were performed at three digit representation sites in areas 3a, 3b, and 1/2, as well as one site in an area 3b face control region. In new world monkey, digit representations are organized in a tip to tip manner in areas 1 and 2, therefore, it is hard to separate which area digit tip belongs to each ROI in our experimental setting. We thus used area 1/2 to infer the ROI in these two regions. Before recording, manual palpation with light tapping stimuli was used to map receptive fields representing the hand, digits, and face. The receptive fields of neurons isolated at each penetration site were measured and recorded. Spontaneous broadband LFP signals and multiunit activity were recorded simultaneously from these four sites with a Plexon multichannel recording system (Plexon, Inc.). Thirty-three 10-min long recording trials were included in

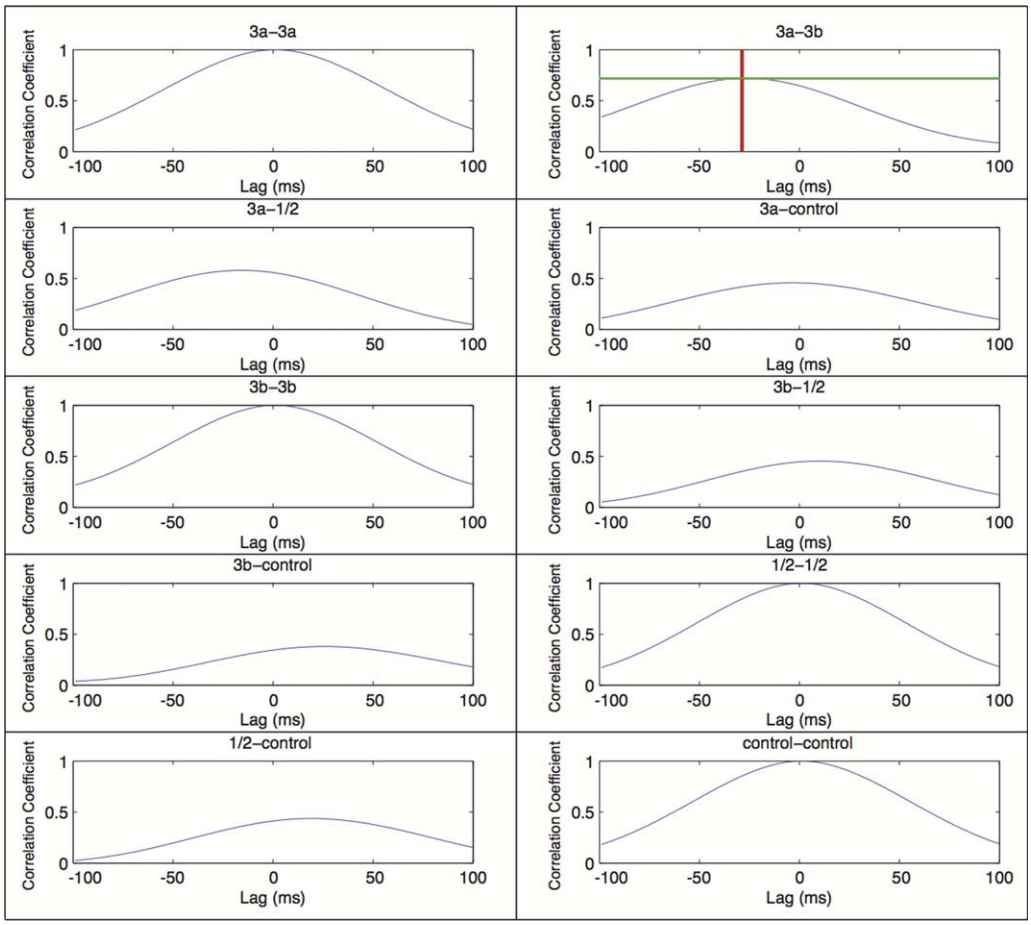

Figure 2.

Representative correlation coefficient and lag plots of instantaneous amplitudes of different ROI pairs from one subject. This figure shows correlation coefficient plots of the delta (1–4 Hz) power band of instantaneous amplitudes populated via the Hilbert transform (Adhikari et al., 2010). The title of each plot displays the ROI pair, the y-axis is the correlation coefficient, and the x-axis is the temporal offset (lag) between the area pairs. The areas 3a and 3b graph shows an example measurement of a maximum amplitude and lag between an electrode pair. The horizontal line shows areas 3a and 3b have a maximum correlation coefficient of 0.76, and the vertical line shows area 3a leading area 3b by 29 milliseconds (ms). As a control, the autocorrelations (e.g., 3a–3a, 3b–3b, etc.) all show correlation coefficients of one and lag of zero ms. [Color figure can be viewed in the online issue, which is available at wileyonlinelibrary.com.]

the analysis. Only LFP data were analyzed and are reported here. LFP signals were filtered into seven frequency bands: delta (1–4 Hz), theta (5–8 Hz), alpha (9–14 Hz), beta (15–30 Hz), gamma low (31–50 Hz), gamma high (51–100 Hz), and gamma very high (100–150 Hz). These seven frequency bands, as well as the broadband (1–150 Hz) LFP signals, were then analyzed via the method of Adhikari et al. [2010], which applies a Hilbert transform to the LFP signals. With this method, two parameters were derived: cross-correlation coefficients of instantaneous amplitude ($-1 \leq r \leq 1$) and temporal lag (in milliseconds). The instantaneous amplitude of the LFP signal was computed using the MATLAB function *Hilbert*; the correlation of instantaneous amplitude is a common measure for quantifying functional connectivity [Srinath and Ray, 2014]. The instantaneous amplitudes for each electrode were then cross-correlated as area pairs (e.g., 3a–3b vs. 3a–A1). Figure 2 shows an example of cross-correlation line results in which the peak amplitude represents the magnitude of the correlation coefficient between area pairs and the location of the peak represents the lag between the areas. Dunn's multiple comparison test was used to compare the mean rank of each area pair that was obtained from Friedman's test, a non-parametric statistical test similar to the repeated measures ANOVA, in GraphPad Prism version 5.04 for Windows (GraphPad Software).

RESULTS

Differential Correlations of Resting State BOLD fMRI Signals among S1 Sub-Regions

To illustrate the overall inter-areal correlation patterns of resting state fMRI signals, we first plotted voxel-wise correlation maps of seeds placed in area 3b digit (blue dots in Fig. 1C, E) and control face regions (blue dots in Fig. 1C, F) in two monkeys. Seed locations were selected based on the representation maps of digits and face, which were determined by the neuronal receptive field properties (see color dots in Fig. 1. Each dot represents one penetration site). When a seed (blue dots in Fig. 1C and E) was placed in a voxel that corresponded with an electrode penetration site that responded to tactile stimulation of digit 3, significantly correlated signal changes were detected in adjacent voxels within area 3b, and digit 3 regions in areas 3a and 1/2 (threshold $r > 0.5$). In both cases, the overall correlation patterns were quite similar, with strong correlations among corresponding digits regions.

To examine the specificity of the inter-areal fMRI correlation pattern, we compared the correlation maps of area 3b seeds in the digit region with those in the face region (comparing Fig. 1C,E with Fig. 1D,F). Seeds in the face region serve as good built-in controls for the digit regions since it is known that these two regions have no direct functional or anatomical connections [Fang et al., 2002]. The control face seed exhibited strong functional connectivity (high correlations) around the seed voxel, with little to no correlations with the digit regions in areas 3a, 3b, and 1/2. The above described functional connectivity patterns were observed across animals and are consistent with our previous observations [Chen et al., 2011; Wang et al., 2013]. To understand whether there are functional connectivity differences among S1 sub-regions, we quantified the strengths of pair-wise inter-regional correlations (r values) and Figure 1B summarizes the findings across four regions. Equally strong correlations among the digit regions of areas 3a, 3b, and 1/2 were observed. The correlation coefficients were 0.64 ± 0.04 between area 3a and area 3b (3a–3b), 0.60 ± 0.03 between area 3a and area 1/2 (3a–A1) and 0.59 ± 0.03 between area 3b and area 1/2 (3b–A1). The functional connectivity between the digit and face regions was significantly weaker than those between digit regions.

S1 Sub-Regions Exhibited Different Inter-Regional Correlation Amplitudes in Specific Bands of Resting State LFP Signals

Using the same seed ROI pairs as the rsfMRI analysis, we examined the differences in inter-areal correlation strength of different bands of LFP signals (after Hilbert transformation) among S1 sub-regions. A graphical example of the measures of cross correlation between instantaneous amplitudes and values of lag (in milliseconds) of LFP signals derived for each ROI pair can be seen in Figure 2. Figure 3 shows the peak inter-areal correlation differences at each specific frequency band and for the broadband LFP signal. Statistically different correlations between digit–digit S1 sub-region pairs and digit–face control pairs were detected in the broadband LFP signals and all LFP bands, with the exception of the theta band (Fig. 3; Dunn's multiple comparison test: $P < 0.05$, $P < 0.001$, $P < 0.001$). These differences in correlation strengths mimic the fMRI data (compare Fig. 3 with Fig. 1B). There were no significant differences within the three digit–digit or the three digit–face control pairs in any frequency band.

Direct Comparison of Inter-Areal Functional Connectivity Revealed by Resting State fMRI and LFPs

To understand the relationships between the inter-areal functional connectivity indicated by resting state fMRI and specific bands of local field potential, we combined measures of digit representations in S1 sub-regions and digit–control pairs to compare them directly (Fig. 4). Similar rsfMRI connectivity differences between digit–digit and digit–face control ROI pairs were present in delta, alpha, and gamma LFP bands. It is clear that for both measures, digit representations in S1 sub-regions exhibited much stronger functional connectivity with each other than with the control face region in area 3b. The differences, however, were more robust with rsfMRI than LFP signals.

LFP Temporal Lag Reveals Directional Information among S1 Sub-Regions

We next examined if there was any evidence for directionality of information flow between the sub-regions of S1; the results are presented in Figure 5. A negative lag in an area 3a–3b pair, for example, indicates that the area 3a leads area 3b (Fig. 2). Area 3a led area 3b in alpha, beta, gamma low, and gamma very high bands. Area 3a also led area 1/2 in the delta, alpha, beta, and gamma low bands. The relationship between area 3b and area 1/2 shows a bidirectionality of information flow. Area 3b led area 1/2 in the alpha, gamma low, and gamma very high bands; however, area 3b lagged area 1/2 in the beta band.

DISCUSSION

The Use of a Non-Human Primate Model for Studying Functional Connectivity

The non-human primate brain is an ideal experimental model to study the neuronal basis of resting state fMRI signals because it closely resembles the organization of the human brain, from which both fMRI and electrophysiological data via invasive means can be obtained from the same neural network and compared directly [Leopold

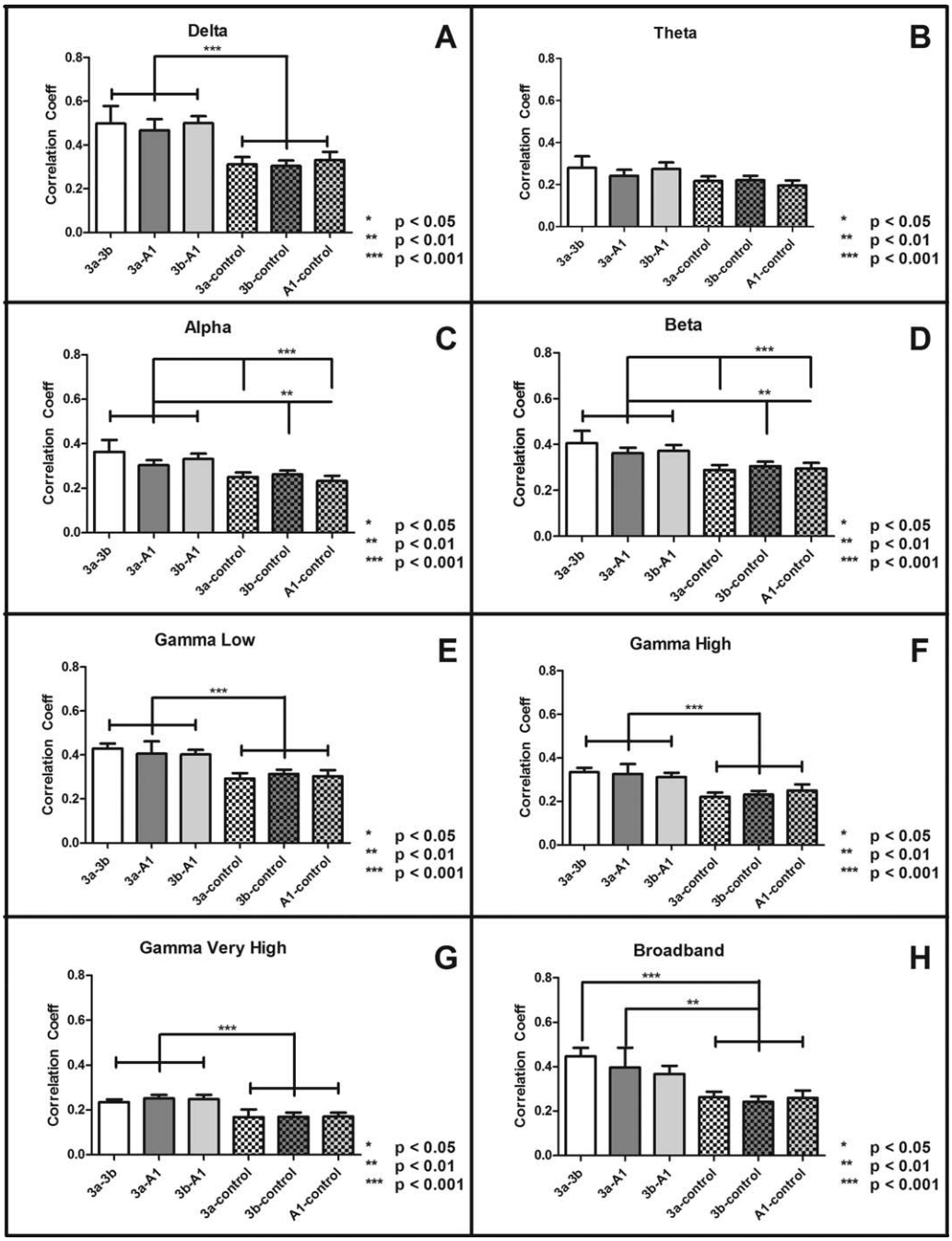

Figure 3.

Inter-areal correlation coefficients of spontaneous LFP signals in different frequency bands across different ROI pairs. (**A–H**) Bar plots of peak inter-areal correlation coefficients (*r* values) of six ROI pairs in delta (A), theta (B), alpha (C), beta (D), gamma low (E), gamma high (F), gamma very high (G), and broad (H) frequency bands. Error bars indicate standard error of the mean (SEM; $N = 33$). Differences between inter-areal connections calculated via Dunn's multiple comparison test post Friedman's test, ($^{*}P < 0.05$, $^{**}P < 0.001$, $^{***}P < 0.001$). All LFP bands, with the exception of the theta band, displayed similar correlation profiles as fMRI data presented in Figure 1B.

et al., 2003; Leopold and Maier, 2012]. We [Wang et al., 2013] and other research groups have previously demonstrated the power of such an approach [Attwell and Iadecola, 2002; Hutchison and Everling, 2012; Iadecola and Nedergaard, 2007; Raichle and Mintun, 2006; ; Uludağ et al., 2004]. In the current study, we identified distinct intrinsic functional connections between digit and face regions in different sub-regions (i.e., areas 3a, 3b, and 1) of the primary somatosensory cortex (S1) of squirrel monkeys [Wang et al., 2013]. This network represents a small mesoscale (defined as at a spatial resolution of hundreds of micrometers and captures anatomically and/or functionally distinct neuronal populations, formed by local circuits [e.g., single digit cortical columns] that link hundreds or thousands of individual neurons) local network within the S1 cortex. We provided evidence for the existence of heterogeneous local functional networks within S1 cortex of primates. Our finding indicates that it is necessary to consider the functional homogeneity of the cortical regions when performing functional connectivity studies in humans.

Similar Inter-Areal Correlation Patterns of Low-Middle Frequency Range of LFP and Resting State fMRI Signals

In the present study, we examined the relationship between the inter-regional rsfMRI connectivity and the inter-regional connectivity of local field potentials. We first confirmed our previous findings with rsfMRI signals and found greater functional connectivity between S1 sub-regions representing the digit than between S1 digit and a control face region. By using the same sets of seeds used in rsfMRI analysis for LFP recordings in each animal, we were able to compare directly the inter-areal correlation differences revealed by rsfMRI and resting state LFPs. We found that correlations in certain LFP frequency bands between S1 digit sub-regions, but not others, were significantly greater than those between digit–face control region (Fig. 4). Our findings agree with previous work that indicates neurons that share receptive fields and process the same inputs also fluctuate coherently at rest [Wang et al., 2013]. Extending previous observations with rsfMRI and multiunit recordings, here we demonstrated that cortical regions that showed strong rsfMRI connectivity also exhibited strong correlated fluctuations of local field potentials in low to middle frequency ranges (1–50 Hz). These results agree with other resting state studies that have shown the delta band to be predictive of BOLD signal [Lu et al., 2007; Pan et al., 2013; Wang et al., 2012], as well as those that point to the gamma band [He et al., 2008; Niessing et al., 2005; Nir et al., 2007, 2008]. In fact, our evidence for the comparable differences in inter-areal correlation strengths between rsfMRI and resting state LFP measures speaks strongly for a neuronal basis of resting state fMRI signal fluctuations. The existence of the resting state functional

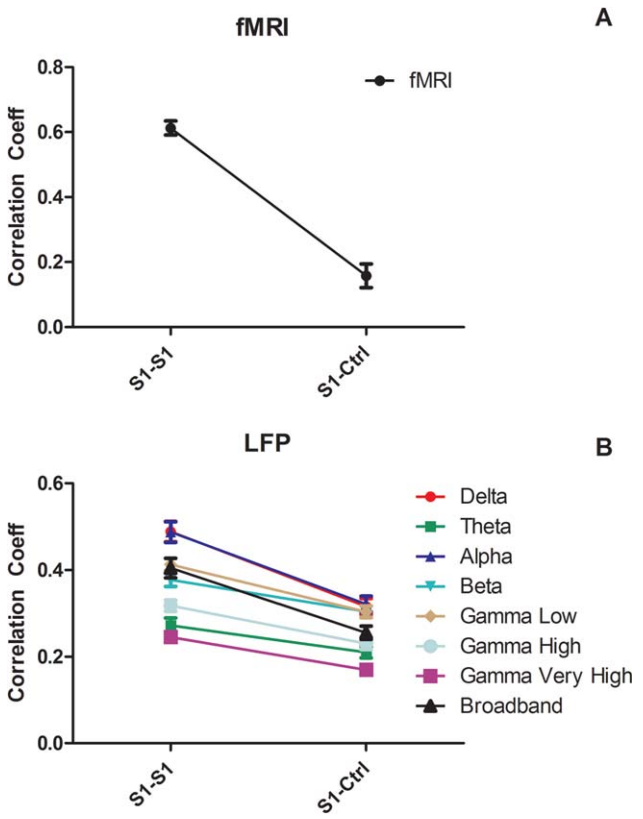

Figure 4.

Inter-areal rsfMRI connectivity covaries with inter-areal correlations of delta, alpha, and gamma low band LFPs signals within the S1 cortex of squirrel monkeys. Functional connectivity measures between sub-regions of digit representation within S1 (S1–S1) are more highly correlated than those between S1 digit and face (S1–Ctri) control region for rsfMRI and all but the theta band of LFP. Error bars indicate SEM ($N = 33$). [Color figure can be viewed in the online issue, which is available at wileyonlinelibrary.com.]

connectivity network within such a small local region of S1 cortex calls for extra caution in interpreting negative findings in studies aimed to explore rsfMRI connectivity network of human S1 cortex, because often in those studies the S1 cortex was studied as one cortical entity [Cordes et al., 2000, 2001; DeLuca et al., 2005]. Partial volume effects (e.g., inclusion of different parts of the network) may contribute to the variation of rsfMRI signal acquired.

We attribute our successful detection of functional connectivity differences between digit–digit and digit–face pairs within S1 cortex to the high signal- and contrast-noise ratio at high MRI field, as well as our analysis strategy of the use of a single voxel seed. The choice of a single voxel for rsfMRI data analysis is based on our previous observations and the functional organizational feature of the cortical region we studied (digit and face representations). We found previously that higher functional

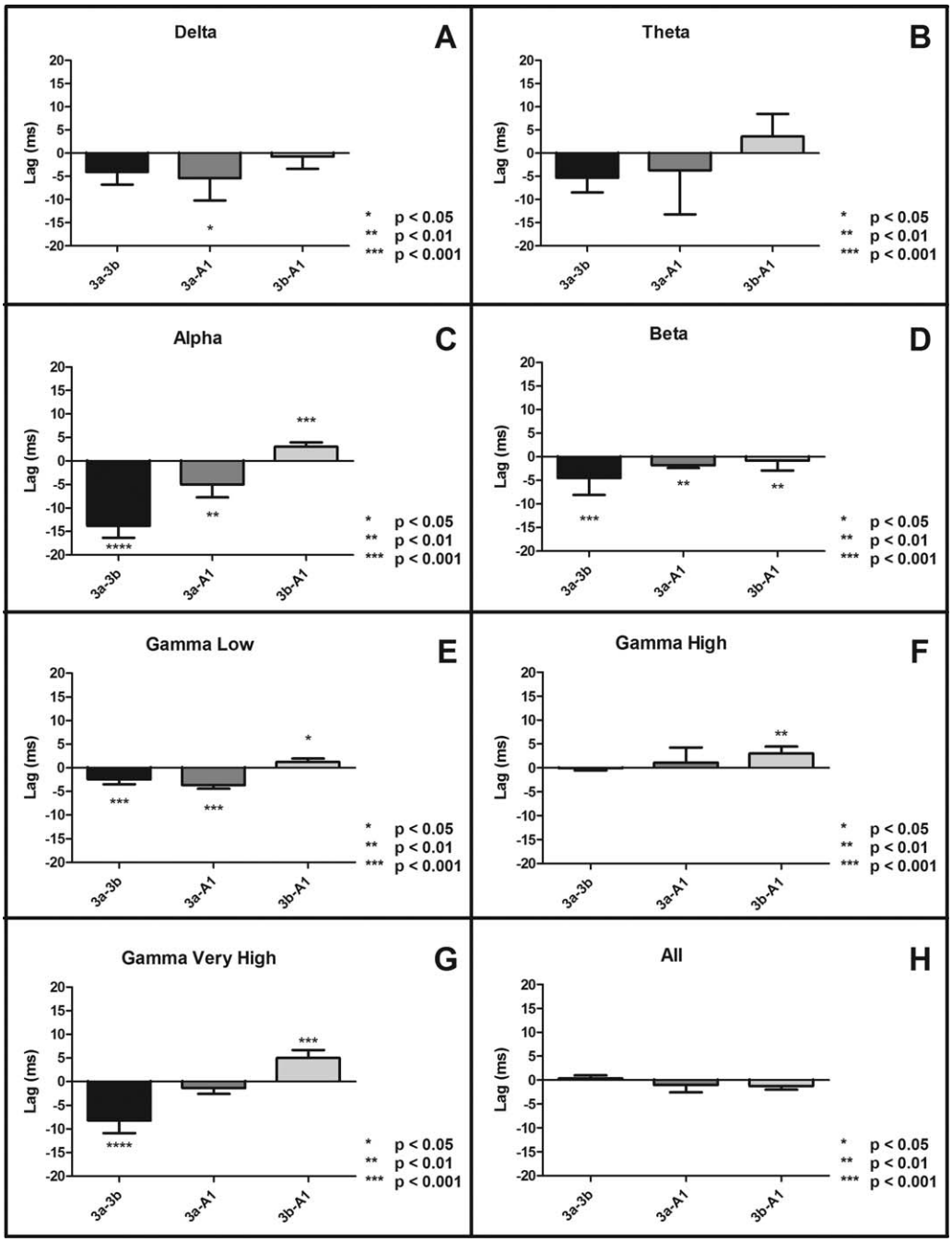

Figure 5.

Temporal lag of peak instantaneous amplitudes of cross-correlograms between seed areas of different ROI pairs. (**A–D**) Plots of lags between digit representations in sub-regions of S1 in four different LFP frequency bands. A negative lag indicates that the first area leads the second area. Differences between inter-areal connections were calculated via a Wilcoxon signed-rank test, (*$P < 0.05$, **$P < 0.001$, ***$P < 0.001$). Error bars represent SEM ($N = 33$).

homogeneity of neurons within each ROI exhibits stronger correlation. In this study, we focused on single digit representation, which is about 1.5 × 1.5 mm^2 in area 3b and smaller in areas 3a and 1. In this context, 1–2 single voxel (0.57 × 0.57 mm^2 in plan) is about 1/2 to 1/3 of the single digit representation. We, therefore, used a single voxel in

our analysis to minimize the partial volume effect. Another note is that the physical distance between ROIs reduces their spontaneous correlation strength [Genc et al., 2015]. However, we do not think this is driving our observed correlation difference between digit–digit and digit–face control ROI pairs because the actual distances between digit regions across areas within S1 (e.g., ~3–4 mm between area 3a and area 1/2) were comparable to average digit–face distance (e.g., ~1 mm between digit 1 and face, and 5 mm between digit 5 and face) ROI pairs. Taken together, our data indicate that power correlations within certain frequency bands (1–50 Hz) underlie the neuronal correlates of resting-state functional connectivity.

The Behavioral Relevance of the Correlated LFP Signals

The known behavioral significance and physiological functions of the LFP bands presented here provide new insights into the interpretation of the functional connectivity we observed in the current study. For example, although the origin of the delta rhythm is unclear, it has been implicated in slow-wave sleep in humans [Steriad, 2000]. Delta oscillations have also been reported to have an organizing influence on sensory processing [Lakatos et al., 2008]. One proposed explanation for this slow coordinated activity is that it acts as maintenance of synaptic connections between structurally interconnected neurons representing the digit in S1 [Leopold and Maier, 2012; Schroeder and Lakatos, 2008; Steriade, 2006]. This synaptic maintenance may explain the high level of coherence in the delta band shown in the resting state condition.

The differential correlations detected in the alpha band likely stem from driving thalamic inputs into S1 (see our proposed model in Fig. 6). All sub-regions explored in this study receive direct inputs (to various degrees) from the ventral posterolateral nucleus (VPL) of the thalamus [Friedman and Jones, 1981], and thalamic activity has been implicated in coordination of cortical alpha band activity [Hughes and Crunelli, 2007; Hughes et al., 2004; Palva and Palva, 2011]. It has been shown that active processing in early sensory regions (to which S1 belongs) is associated with decreased alpha amplitudes [Bollimunta et al., 2008, 2011; Palva and Palva, 2011]. It is believed that alpha oscillations are inversely associated with gamma band activity, the former acting as a sensory gating mechanism with periodic excitability fluctuations to accommodate the sensory information carried by the latter [Mo et al., 2011]. Thus, it stands to reason that baseline alpha band activity would show significant correlations between areas with similar sensory input in the absence of stimuli. The comparatively low correlations in the gamma bands are likely explained through this mechanism as well, and are indicative of the resting state condition. We would expect alpha correlations to decrease and gamma low correlations to increase among digit areas in S1 sub-regions in the presence of stimuli [Kilner et al., 2005]. Another possibility for the role of the correlations in the gamma bands in this study relates to its role in top-down processing of sensory stimuli [Bauer et al., 2006]. These LFP findings in S1 cortex are in line with previous resting state LFP/fMRI observations in visual cortex [Scholvinck et al., 2010; van Kerkoerle et al., 2014], with the exception of the beta band. Beta band correlations have been identified between S1 and primary motor (M1) cortices [Murthy and Fetz, 1992]. The presence of beta band correlations within digit representations of S1 sub-regions here supports its role in coordinating sensorimotor processes.

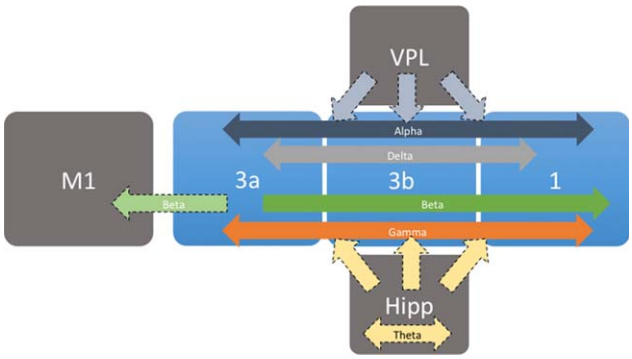

Figure 6.
Summary of functional connectivity between digit representations in S1 sub-regions. *Arrows* indicate the directionality of the information flow. *Dark arrows* represent findings from this study; *lighter dotted arrows* represent proposed directionality based on previous work. [Color figure can be viewed in the online issue, which is available at wileyonlinelibrary.com.]

Implications of Lag Difference in Resting LFP Signal within S1 Subregions

The temporal lag information provided by the Hilbert transform allowed us to investigate the direction of information flow between the digit representations in subregions of S1 at rest (Fig. 5). Within S1 cortex, area 3b and area 1 are primary regions for processing low threshold discriminative tactile information, whereas area 3a and area 1/2 are more involved in processing proprioceptive information [Kaas, 1983]. We found that area 1 lagged behind area 3a in four LFP frequency bands that showed significant correlation between areas of digit representation in S1 (i.e., delta, alpha, beta, gamma low). In primates, area 1 has more complex receptive field properties than neurons in areas 3a or 3b [Iwamura et al., 1983], and cortico-cortical connections between these S1 sub-regions have been identified [Guldin et al., 1992]. These findings suggest converging inputs from area 3a to area 1, presumably allowing for different aspects of somatotopic integration (e.g., proprioception) for the digit [Krubitzer and Kaas, 1990].

Significantly different temporal lags were revealed in the beta and gamma bands, in which area 3a led area 3b. This suggests that different frequency bands at rest may participate in different brain functions. While anatomical connections from area 3b to 3a are well established, reciprocal connections are uncommon [Darian-Smith et al., 1993; Jones et al., 1978]. Since 3a efferent connections to 3b are likely not responsible for the lag of information flowing from area 3a to area 3b, we propose that common inputs into these areas may explain our results in the beta and gamma bands. Strong, somatotopically organized connections exist between all sub-regions of S1 and M1 in monkey [Stepniewska et al., 1993], where sensorimotor beta oscillations have been shown [Baker et al., 1997; Murthy and Fetz, 1996]. The spatial coexistence of beta and gamma oscillations in S1 has been previously reported [Roopun et al., 2006]. Oscillations in the gamma band of the LFP signal have been implicated in tactile spatial attention [Bauer et al., 2006], pain perception [Zhang et al., 2012], and stimulus intensity encoding [Rossiter et al., 2013]. More broadly, gamma band synchrony is thought to reflect localized top-down computations of behaviorally relevant stimuli in small networks [Engel et al., 2001; Fries et al., 2007; Montgomery and Buzsaki, 2007; Pesaran et al., 2002; Schoffelen et al., 2005; Fukushima et al., 2012]. In the absence of stimuli, hippocampal rhythms have been shown to modulate gamma band activity in neocortex [Sirota et al, 2008; Wyart and Tallon-Baudry, 2008], perhaps acting as another gating mechanism for sensory information [Bland, 1986]. The top-down nature of the gamma oscillations may explain the information flow from area 3a to area 3b.

The beta and low gamma bands in this study illustrate a bidirectionality of information flow between areas 3b and 1: area 3b led area 1 in the beta band, but lagged behind area 1 in the gamma bands. The difference in information flow in these bands may be related to the extensive and reciprocal connections that have been found between areas 3b and 1 [Burton and Fabri, 1995; DeFelipe et al., 1986; Jones and Powell, 1969; Shanks et al., 1985; Négyessy et al., 2013; Ashaber et al., 2014]. There is also strong anatomical evidence for serial information processing between area 3b and area 1 [Cusick et al., 1985; Jones and Wise, 1977; Vogt and Pandya, 1978], with area 1 being a high-order region receiving inputs from area 3b [Iwamura et al., 1993; Iwamura, 1998]. This has led many to consider area 1 as a higher order somatosensory cortex, as response in area 1 is dependent on intact area 3b [Garraghty et al., 1990; Pons et al., 1992] especially for noxious stimuli [Chudler et al., 1990; Kenshalo and Willis, 1991; Kenshalo et al., 2000]. However, given the relationship between areas 3a and 3b, it is possible that hippocampal and motor inputs mentioned above are driving these flows of information. Beta oscillations measured in this study originate in 3a and reach area 1 after being delivered to 3b. This fits with previous work in primates showing beta oscillations within sensorimotor loops originating in S1 and traveling separately to M1 and other postcentral cortical areas [Brovelli et al., 2004].

In conclusion, by using inter-regional correlation strengths within S1 cortex as measures of functional connectivity, we found strong relationships between the correlations in resting state fMRI fluctuations and corresponding correlations between the low- to middle-range LFP signals. The differential correlation strengths between digit–digit versus digit–face control regions support the existence of fine-scale local functional networks within S1 cortex. This observation gives reason to exercise caution in interpreting negative detections of resting state functional connectivity between S1 cortex and other cortical or subcortical regions, given the heterogeneity of the functional network organization revealed in this study.

ACKNOWLEDGMENT

The authors gratefully acknowledge Dr. Baxter Rogers for his advice on LFP signal processing and Chaohui Tang for her assistance on data collection.

REFERENCES

Adhikari A, Sigurdsson T, Topiwala MA, Gordon JA (2010): Cross-correlation of instantaneous amplitudes of field potential oscillations: A straightforward method to estimate the directionality and lag between brain areas. J Neurosci Methods 191: 191–200.

Attwell D, Iadecola C (2002): The neural basis of functional brain imaging signals. Trends Neurosci 25:621–625.

Baker SN, Olivier E, Lemon RN (1997): Coherent oscillations in monkey motor cortex and hand muscle EMG show task-dependent modulation. J Physiol Lond 501:225–241.

Bauer M, Oostenveld R, Peeters M, Fries P (2006): Tactile spatial attention enhances gamma-band activity in somatosensotry cortex and reduces low-frequency activity in parieto-occipital areas. J Neurosci 26:490–501.

Bisal B, Yetkin FZ, Haughton VM, Hyde JS (1995): Functional connectivity in the motor cortex of resting human brain using echo-planar MRI. MR Med 34:537–541.

Bland BH (1986): The physiology and pharmacology of hippocampal formation theta rhythms. Prog Neurobiol 26:1–54.

Bollimunta A, Chen Y, Schroeder CE, Gind M (2008): Neuronal mechanisms of cortical alpha oscillations in awake-behaving macaques. J Neurosci 28:9976–9988.

Bollimunta A, Mo J, Schroeder CE, Ding M (2011): Neuronal mechanisms and attentional modulation of corticothalamic alpha oscillations. J Neurosci 31:4935–4943.

Brovelli A, Ding M, Ledberg A, Chen Y, Nakamura R, Bressler S (2004): Beta oscillations in a large-scale sensorimotor cortical network: Directional influences revealed by Granger causality. PNAS 101:9849–9854.

Burton H, Fabri M (1995): Ipsilateral intracortical connections of physiologically defined cutaneous representations in areas 3b and 1 of macaque monkets: Projections in the vicinity of the central sulcus. J Compar Neurol 355:508–538.

Chen LM, Mishra A, Newton AT, Morgan VL, Stringer EA, Rogers BP, Gore John C (2011): Fine-scale functional connectivity in

somatosensory cortex revealed by high-resolution fMRI. Magnetic Resonance Imaging 29:1330–1337.
Chudler EH, Anton F, Dubner R, Kenshalo DRJ (1990): Responses of nociceptive S1 neurons in monkeys and pain sensation in humans elicited by noxious thermal stimulation: Effect of interstimulus interval. J Neurophysiol 63:559–569.
Cordes D, Haughton VM, Arfanakis K, Wendt GJ, Turski PA, Moritz CH, Quigley MA, Meyerand ME (2000): Mapping functionally related regions of brain with functional connectivity MR imaging. Am J Neuroradiol 21:1636–1644.
Cordes D, Haughton VM, Arfanakis K, Carew JD, Turski PA, Moritz CH, Quigley MA, Meyerand ME (2001): Frequencies contributing to functional connectivity in the cerebral cortex in "resting-state" data. Am J Neuroradiol 22:1326–1333.
Cusick CG, Steindler DA, Kaas JH (1985): Corticocortical and collateral thalamocortical connections of postcentral somatosensory cortical areas in squirrel monkeys. Somatosens Res 3:1–31.
Damoiseaux JS (2012): Resting-state fMRI as a biomarker for Alzheimer's disease? Alzheimer's Res Ther 4:8.
Darian-Smith C, Darian-Smith I, Kathleen B, Ratcliffe N (1993): Ipsilateral cortical projections to areas 3a, 3b, and 4 in the macaque monkey. J Comp Neurol 335:200–213.
Deco G, Corbetta M (2011): The dynamical balance of the brain at rest. Neuroscientist 17:107–123.
Deco G, Jirsa VK, McIntosh AR (2011): Emerging concepts for the dynamical organization of resting-state activity in the brain. Nat Rev Neurosci 12:43–56.
DeFelipe J, Conley M, Jones EF (1986): Long-range focal collateralization of axons arising from corticortical cells in monkey sensory-motor cortex. J Neurosci 6:3749–3766.
DeLuca M, Smith S, DeStefano N, Federico A, Matthews PM (2005): Blood oxygenation level dependent contrast resting state networks are relevant to functional activity in the neocortical sensorimotor system. Exp Brain Res 167:587–594.
Engel AK, Fries P, Singer W (2001): Dynamic predictions: Oscillations and synchrony in top-down processing. Nat Neurosci 2: 704–716.
Fang PC, Jain N, Kaas JH (2002): Few intrinsic connections cross the hand-face border of area 3b of New World monkeys. J Comp Neurol 454:310–319.
Fingelkurts AA, Kahkonen S (2005): Functional connectivity in the brain: Is it an elusive concept? Neurosci Biobehav Rev 28:827–836.
Fox MD, Raichle ME (2007): Spontaneous fluctuations in brain activity observed with functional magnetic resonance imaging. Nat Rev Neurosci 8:700–711.
Fox MD, Greicius M (2010): Clinical applications of resting state functional connectivity. Front Sys Neurosci 4:19.
Friedman DP, Jones EG (1981): Thalamic Input to areas 3a and 2 in monkeys. J Neurophysiol 45:59–64.
Fries P, Nikolic D, Singer W (2007): The gamma cycle. Trends Neurosci 30:306–316.
Fukushima M, Saunders RC, Leopold DA, Mishkin M, Averbeck BB (2012): Spontaneous high-gamma band activity reflects functional organization of auditory cortex in the awake macaque. Neuron 74:899–910.
Garraghty PE, Florence SL, Kaas JH (1990): Abalations of areas 3a and 3b of monkey somatosensory cortex abolish cutaneous responsivity in area 1. Brain Res 528:165–169.
Genc E, Scholvinck ML, Bergmann J, Singer W, Kohler A (2015): Functional connectivity patterns of visual cortex reflect its anatomical organization. Cereb Cortex pii:bhv175.
Glover GH, Li TQ, Ress D (2000): Image-based method for retrospective correction of physiological motion effects in fMRI: RETROICOR. Magn Res Med 44:162–167.
Greicius MD, Krasnow B, Reiss AL, Menon V (2002): Functional connectivity in the resting brain: A network analysis of the default mode hypothesis. Proc Natl Acad Sci USA 100:253–258.
Guldin WO, Akbarian S, Grusser OJ (1992): Cortico-cortical connections and cytoarchitectonics of the primate vestibular cortex: A study in squirrel monkeys (*Saimiri sciureus*). J Comp Neurol 326:375–401.
Gusnard DA, Raichle ME (2001): Searching for a baseline: Functional imaging and the resting state brain. Nat Rev Neurosci 2:685–694.
Guye M, Bartolomei F, Ranjeva JP (2008): Imaging structural and functional connectivity: Towards a unified definition of the human brain organization? Curr Opin Neurol 21:393–403.
He BJ, Snyder AZ, Zempel JM, Smyth MD, Raichle ME (2008): Electrophysiological correlates of the brain's intrinsic large-scale functional architecture. Proc Natl Acad Sci USA 105: 16039–16044.
Hughes SW, Crunelli V (2007): Just a phase they're going through: The complex interaction of intrinsic high-threshold busrting and gap junctions in the generation of thalamic alpha and theta rhythms. Int J Psychophys 64:3–17.
Hughes SW, Lorincz M, Cope DW, Blethyn KL, Kekesi KA, Parri HR, Juhasz G, Crunelli V (2004): Synchronized oscillations at alpha and theta frequencies in the lateral geniculate nucleus. Neuron 42:253–268.
Hutchison RM, Everling S (2012): Monkey in the middle: Why non-human primates are needed to bridge the gap in resting-state investigations. Front Neuroanat 6:1–19.
Iadecola C, Nedergaard M (2007): Glial regulation of the cerebral microvasculature. Nat Neurosci 10:1369–1376.
Iwamura Y (1998): Hierarchical somatosensory processing. Curr Opin Neurobiol 8:522–528.
Iwamura Y, Tanaka M, Sakamoto M, Hikosaka O (1983): Converging patterns of finger representation and complex response properties of neurons in area 1 of the first somatosensory cortex of the conscious monkey. Exp Brain Res 51:327–337.
Iwamura Y, Tanaka M, Sakamoto M, Hikosaka O (1993): Rostrocaudal gradients in the neuronal receptive field complexity in the finger region of the alert monkey's postcentral gyrus. Exp Brain Res 51:327–337.
Jones EG, Powell TPS (1969): Connexions of the somatic sensory cortex of the rhesus monkey I Ipsilateral cortical connexions. Brain 92:477–502.
Jones EG, Wise SP (1977): Size, laminar and columnar distribution of efferent cells in the sensory-motor cortex of monkeys. J Comp Neurol 175:391–438.
Jones EG, Coulter JD, Hendry SHC (1978): Intracortical connectivity of architectonic fields in the somatic sensory, motor and parietal cortex of monkeys. J Comp Neurol 181:291–348.
Kaas JH (1983): What, if anything, is S-I? Organization of first somatosensory area of cortex. Physiol Rev 63:206–231.
Kenshalo DR Jr, Willis WD Jr (1991): The role of the cerebral cortex in pain sensation. In: Jones EG, Peters A, editors. Cerebral Cortex. New York: Plenum. pp 151–212.
Kenshalo DRJ, Iwata K, Sholas M, Thomas DA (2000): Response properties and organization of nociceptive neurons in area 1 of monkey primary somatosensory cortex. J Neurophysiol 84:719–729.
Kilner J, Bott L, Posada A (2005): Modulations in the degree of sunchronization during ongoing oscillatory activity in the human brain. Eur J Neurosci 21:2547–2554.

Krubitzer LA, Kaas JH (1990): The organization and connections of somatosensory cortex in marmosets. J Neurosci 10:952–974.

Lakatos P, Karmos G, Mehta AD, Ulbert I, Schroeder CE (2008): Entrainment of neuronal oscillations as a mechanism of attentional selection. Science 320:110–113.

Leopold DA, Maier A (2012): Ongoing physiological processes in the cerebral cortex. NeuroImage 62:2190–2200.

Leopold DA, Murayama Y, Logothetis NK (2003): Very slow activity fluctuations in monkey visual cortex: Implications for functional brain imaging. Cereb Cortex 13:422–433.

Logothetis NK, Pauls J, Augath M, Trinath T, Oeltermann A (2001): Neurophysiological investigation of the basis of the fMRI signal. Nature 412:150–157.

Lu H, Zuo Y, Gu H, Waltz JA, Zhan W, Scholl CA, Rea W, Yang Y, Stein EA (2007): Synchronized delta oscillations correlate with the resting-state functional MRI signal. Proc Natl Acad Sci USA 104:18265–18269.

Mo J, Schroeder CE, Ding M (2011): Attentional modulation of alpha oscillations in macaque inferotemporal cortex. J Neurosci 31:878–882.

Montgomery SM, Buzsaki G (2007): Gamma oscillations dynamically couple hippocampal CA3 and CA1 regions during memory task performance. Proc Natl Acad Sci USA 104:14495–14500.

Mukamel R, Gelbard H, Arieli A, Hasson U, Fried I, Malach R (2005): Coupling between neuronal firing, field potentials, and fMRI in human auditory cortex. Science 309:951–955.

Murthy VN, Fetz EE (1992): Coherent 25- to 35-Hz oscillations in the sensorimotor cortex of awake behaving monkeys. Proc Natl Acad Sci USA 89:5670–5674.

Murthy VN, Fetz EE (1996): Oscillatory activity in sensorimotor cortex of awake monkeys: Synchronization of local field potentioals and relation to behavior. J Neuropyshiol 76:3949–3967.

Negyessy L, Palfi MA, Palmer C, Jakli B, Friedman RM, Chen LM, Roe AW (2013): Intrinsic horizontal connections process global tactile features in the primary somatosensory cortex: neuroanatomical evidence. Journal of Comparative Neurology 521:2798–2817.

Niessing J, Ebisch B, Schmidt KE, Niessing M, Singer W, Galuske RAW (2005): Hemodynamic signals correlate tightly with synchronized gamma oscillations. Science 309:948–951.

Nir Y, Fisch L, Mukamel R, Gelbard-Sagiv H, Arieli A, Fried I, Malach R (2007): Coupling between neuronal firing rate, gamma LFP, and BOLD fMRI us related to interneuronal correlations. Curr Biol 17:1275–1285.

Nir Y, Mukamel R, Dinstein I, Privman E, Harel M, Fisch L, Gelbard-Sagiv H, Kipervasser S, Andelman F, Neufeld MY, Kramer U, Arieli A, Fried I, Malach R (2008): Interhemispheric correlations of slow spontaneous neuronal fluctuations revealed in human sensory cortex. Nat Neurosci 11:1100–1108.

Palva S, Palva JM (2011): Functional roles of alpha-band phase synchronization in local and large-scale cortical networks. Front Psychol 2:1–15.

Pan W, Thompson GJ, Magnuson ME, Jaeger D, Keilholz S (2013): Infraslow LFP correlates to resting-state fMRI BOLD signals. NeuroImage 74:288–297.

Pesaran B, Pezaris JS, Sahani M, Mitra PP, Andersen RA (2002): Temporal structure in neuronal activity during working memory in macaque parietal cortex. Nat Neurosci 5:805–811.

Pons TP, Garraghty PE, Mishkin M (1992): Serial and parallel processing of tactual information in somatosensory cortex of rhesus monkeys. J Neurophysiol 68:518–527.

Raichle ME, Mintun MA (2006): Brain work and brain imaging. Annu Rev Neurosci 29:449–476.

Roopun AK, Middleton SJ, Cunningham MO, Lebeau FEN, Bibbig A, Whittington MA, Traub RD (2006): A B2-frequency (20-30 Hz) oscillation in nonsynaptic networks of somatosensory cortex. Proc Natl Acad Sci USA 103:15646–15650.

Rossiter HE, Worthen SF, Witton C, Hall SD, Furlong PL (2013): Gamma oscillatory amplitude encodes stimulus intensity in primary somatosensory cortex. Front Human Neurosci 7:1–7.

Schoffelen JM, Oostenveld R, Fries P (2005): Neuronal coherence as a mechanism of effective corticospinal interaction. Science 308:111–113.

Scholvinck ML, Maier A, Ye FQ, Duyn JH, Leopold DA (2010): Neural basis of global resting-state fMRI activity. Proc Natl Acad Sci USA 107:10238–10243.

Schroeder CE, Lakatos P (2008): Low-frequency neuronal oscillations as instruments of sensory selection. Trends Neurosci 32: 9–18.

Shanks MF, Pearson RCA, Powell TPS (1985): The ipsilateral cortico-cortical connexions between the cytoarchitectonic subdivisions of the primary somatic sensory cortex in monkey. Brain Res Rev 9:67–88.

Shmuel A, Augath M, Oeltermann A, Logothetis NK (2006): Negative functional MRI response correlates with decreases in neuronal activity in monkey visual area V1. Nat Neurosci 9:569–577.

Sirota A, Montgomery S, Fujisawa S, Isomura Y, Zugaro M, Buzsaki G (2008): Entrainment of neocortical neurons and gamma oscillations by the hippocampal theta rhythm. Neuron 60:683–697.

Srinath R, Ray S (2014): Effect of amplitude correlations on coherence in the local field potential. J Neurophysiol 112:741–751.

Stepniewska I, Preuss TM, Kaas JH (1993): Architectonics, somatotopic organization, and ipsilateral cortical connections of the primary motor area (M1) of owl monkeys. J Comp Neurol 330: 238–271.

Steriad M (2000): Corticothalamic resonance, states of vigilance and mentation. Neuroscience 101:243–276.

Steriade M (2006): Grouping of brain rhythms in corticothalamic systems. Neuroscience 137:1087–1106.

Uludağ K, Dubowitz DJ, Yoder EJ, Restom K, Liu TT, Buxton RB (2004): Coupling of cerebral blood flow and oxygen consumption during physiological activation and deactivation measured with fMRI. Neuroimage 23:148–155.

van Kerkoerle T, Self MW, Dagnino B, Gariel-Mathis MA, Poort J, van der Togt C, Roelfsema PR (2014): Alpha and gamma oscillations characterize feedback and feedforward processing in monkey visual cortex. Proc Natl Acad Sci USA 111:14332–14341.

Vogt BA, Pandya DN (1978): Corticocortical connections of somatic sensory cortex in the rhesus monkey. J Comp Neurol 177:179–192.

Wang L, Saalmann YB, Pinsk MA, Arcaro MJ, Kaster S (2012): Electrophysiological low-frequency coherence and cross-frequency coupling contributes to BOLD connectivity. Neuron 76:1010–1020.

Wang Z, Chen LM, Negyessy L, Friedman RM, Mishra A, Gore JC, Roe AW (2013): The relationship of anatomical and functional connectivity to resting-state connectivity in primate somatosensory cortex. Neuron 78:1116–1126.

Wyart V, Tallon-Baudry C (2008): Neural dissociation between visual awareness and spatial attention. J Neurosci 28:2667–2679.

Zhang ZG, Hu L, Hung YS, Mouraux A, Iannetti GD (2012): Gamma-band oscillations in the primary somatosensory cortex – a direct and obligatory correlate of subjective pain intensity. J Neurosci 32:7429–7438.